Theoretical investigations of ZnO/CdO material – A DFT approach

K. Rackesh Jawaher[1], R. Indirajith[1], S. Krishnan[2]*, S. Bharanidharan[3], R. Robert[4], S. Jerome Das[5]

[1]*Department of Physics, B.S. AbdurRahman Crescent Institute of Science and Technology, Chennai-600048, India*
[2]*Department of Physics, Ramakrishna Mission Vivekananda College (Autonomous), Chennai-600004, India*
[3]*Department of Physics, Bharath Institute of Higher Education and Research, Bharath University, Chennai-600073, India*
[4]*Department of Physics, Government Arts College for Men, Krishnagiri-635001, India*
[5]*Department of Physics, Loyola College, Chennai-600 034, India*
*Corresponding author E-mail: rackeshsa@gmail.com

Abstract

The theoretical investigations of ZnO/CdO material were carried out by using *ab initio* calculations. The bond parameters such as bond lengths, bond angles and dihedral angles were calculated at DFT/B3LYP/LANL2DZ level of theory. The NLO property of the title molecule was calculated using a first order hyperpolarizability calculation. NBO study reveals that the hyperconjucative interactions between the material. Homo-Lumo analysis the charge transfer occurs within the molecule. MEP surface predicts the reactive sites of the present molecule. In addition of Mulliken atomic charges and thermodynamic parameters were also plotted and calculated.

Keywords: *ZnO/CdO; DFT Study; NLO; NBO; MEP.*

1. Introduction

In recent years, many researchers focused on the ZnO composite material. It has several applications such as vacuum fluorescent displays, transparent conductive contacts, solar cells, laser diodes, ultraviolet lasers, thin film transistors, optoelectronic, and piezoelectric applications to surface acoustic wave devices (Chong et al., 2012). Especially ZnO has been recognized as the excellent materials for the photocatalytic process due to their high photosensitivity, non toxic nature and large bandgap (Tsai et al., 2011). It has been well studied as a sensor material to detect most of the reducing gases (Zhang et al., 2009; Wang et al., 2012; Na et al., 2011; Wen et al., 2013). Further, CdO is an important semiconductor with band gap of 2.2 eV (Jayakrishnan & Hodes, 2003; Kanjwal et al., 2009). This is a promising catalyst for optoelectronic applications, viz. transparent electrodes, solar cells, phototransistors, photodiodes and gas sensors. Very few researchers reports on the coupling of zinc oxide with cadmium oxide material (Karami, 2010).

In this study, the DFT method is used for the optimization of molecular structure. In addition the theoretical parameters such as NLO property, NBO analysis and Thermodynamic behavior of the present molecule were calculated and briefly discussed. The *ab initio* calculations of ZnO/CdO material have been investigated in detailed for the first time to the best of authors.

2. Computational details

All calculations were performed from *ab initio* DFT method at B3LYP/LANL2DZ level of basis set using the Gaussian 03W (Frisch et al., 2004) program package, invoking gradient geometry optimization (Schlegel, 1982; Scott & Radom 1996). The NBO analysis was calculated to using the NBO 3.1 program. Thermodynamic parameters were calculated with the help of Thermo.pl software package (Irikura, 2002).

3. Results and discussion

3.1. Molecular geometry

The optimized structure of the ZnO/CdO molecule measured at B3LYP/LANL2DZ level of theory and is shown in Fig. 1a. The DFT/B3LYP method calculates to provide a good quality structure. The optimization process goes smoothly till reached a local minimum after 19 steps as shown in Fig. 1b and Fig. 1c, respectively. The bond parameters such as bond lengths and bond angles values are presented in Table 1.

Table 1: The Bond Parameters of ZnO.CdO

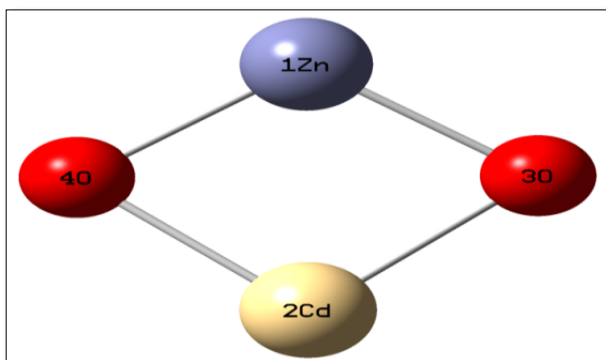| Bond Parameters	
Bond Lengths (Å)	LANL2DZ
Zn1-Cd2	2.5186
Zn1-O3	2.0088
Zn1-O4	2.0088
Cd2-O3	2.1436
Cd2-O4	2.1436
Bond Angles (°)	
O3-Zn1-O4	109.6677
O3-Cd2-O4	100.0065

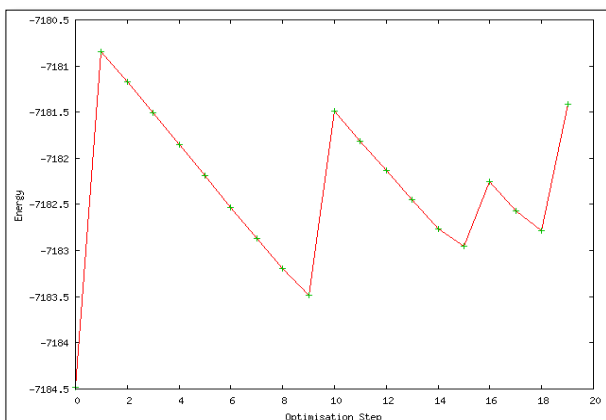**Fig. 1:** a) Optimized Structure of ZnO.CdO.

Fig. 1: b) Optimization Step vs. Energy of ZnO.CdO.
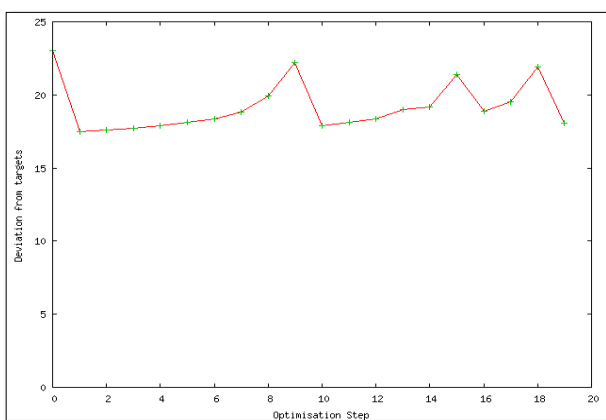

Fig. 1: c) Optimization Step vs. Deviation Targets of ZnO.CdO.

In this study, the Zn1-Cd2 bond length is calculated at 2.5186 Å. This bond length value is higher than that of other bond lengths, which is bonded at metal atoms. The calculation of Zn-O and Cd-O bond distances at 2.0088 and 2.1436 Å, respectively. The bond angles value of O_3-Zn1-O_4 and O3-Cd2-O_4 were calculated at 109.6677 and 100.0065°. This result shows that the title molecule consist the metal ions highly bonded in the title optimized structure.

3.2. Non-linear optics

Non-linear optical (NLO) is the forefront of current research because of its importance in providing key functions of optical modulation, optical switching, optical logic and optical memory for the emerging technologies in areas such as telecommunications, optical interconnections and signal processing (Andraud et al., 1994). The first order hyperpolarizability (β_0) of title molecule is calculated and it is based on the finite-field approach. In the presence of an applied

electric field, the energy of a system is a function of the electric field. Polarizabilities and hyperpolarizabilities characterize the response of a system in an applied electric field (Zhang et al., 2004). First hyperpolarizability is a third rank tensor that can be described by 3x3x3 matrix. The 27 components of the 3D matrix can be reduced to 10 components due to the Klein man symmetry (Kleinman, 1962). The output from Gaussian 03W provides 10 components of this matrix as β_{xxx}, β_{xxy}, β_{xyy}, β_{yyy}, β_{xxz}, β_{xyz}, β_{yyz}, β_{xzz}, β_{yzz} and β_{zzz} respectively. The components of the first-order hyper polarizability can be calculated using the following equations.

$$\mu = (\mu_x^2 + \mu_y^2 + \mu_z^2)^{1/2} \tag{1}$$

$$\alpha_0 = \frac{\alpha_{xx} + \alpha_{yy} + \alpha_{zz}}{3} \tag{2}$$

$$\beta_0 = \left(\beta_x^2 + \beta_y^2 + \beta_z^2 \right)^{1/2} \tag{3}$$

The magnitude of the molecular hyperpolarizability (β_0) is one of important key factors in a NLO system. The B3LYP/LANL2DZ calculated first hyperpolarizability value (β_0) of ZnO.CdO is 2.57815×10^{-30}esu. Therefore, this result concludes that the title molecule is an attractive object for future studies of nonlinear optical properties. The dipole moment (μ), polarizability (α_0) and first order hyperpolarizability (β_0) values are listed in Table 2.

Table 2: The NLO Measurements of ZnO.CdO

Parameters	LANL2DZ
Dipole moment (μ) Debye	
μ_x	0.2619255
μ_y	0.2652029
μ_z	-0.3658893
μ	0.52231 Debye
Polarizability (α_0) x10^{-30}esu	
α_{xx}	76.1528573
α_{xy}	18.5255183
α_{yy}	76.5559266
α_{xz}	-3.175313
α_{yz}	-3.1906681
α_{zz}	43.3139817
α_0	0.16714 x10^{-30}esu
Hyperpolarizability (β_0) x10^{-30}esu	
β_{xxx}	96.9582059
β_{xxy}	40.829434
β_{xyy}	40.6567199
β_{yyy}	98.4009455
β_{xxz}	-36.2293996
β_{xyz}	-18.172736
β_{yyz}	-36.6759870
β_{xzz}	51.3052131
β_{yzz}	51.8811122
β_{zzz}	-56.8678129
β_0	2.57815 x10^{-30}esu

3.3. NBO analysis

The hyper conjugation gives as stabilizing effect that arises from an overlap between an occupied orbital with another neighboring electron deficient orbital, when these orbitals are properly oriented. This non-covalent bonding (anti-bonding) interaction can be quantitatively described in terms of the NBO analysis, which is expressed by means of the second-order perturbation interaction energy ($E^{(2)}$) (Reed & Weinhold, 1983; Reed & Weinhold, 1985; Reed et al., 1985; Foster & Weinhold, 1980). This energy represents the estimate of the off-diagonal NBO Fock matrix elements. It can be deduced from the second-order perturbation approach (Chocholoušová et al., 2004).

$$E^{(2)} = \Delta E_{ij} = q_i \frac{F(i,j)^2}{\varepsilon_j - \varepsilon_i} \tag{4}$$

Where 'qi' is the donor orbital occupancy, 'Σi' and 'Σj' are diagonal elements (orbital energies) and F(i,j) is the off diagonal NBO Fock matrix elements.

The natural bonding orbital (NBO) analysis was calculated at B3LYP/LANL2DZ method using second order perturbation theory. The more energy transfer takes place during π to π* transition rather than σ to σ*. In this study, the present molecule and its orbitals delocalized over the σ-σ* bond. The maximum stabilization energy E$^{(2)}$ associated with hyper conjugative interaction from σZn1-O3 to σ*Zn1-O4 (28.87 KJ/mol) and σZn1-O4 to σ*Zn1-O3 (28.87 KJ/mol), respectively. These corresponding ED/e value is 1.89124e. Generally, lone pair of electronegative atoms have a more energy compared to σ-σ* and π-π* system. But, in our case electro negative atom (Oxygen) have less energy (6.44 KJ/mol), due to the attachment of heavy metals (Zn and Cd). The bonding and anti-bonding orbital energies are listed in Table 3.

Table 3: The NBO Analysis of ZnO.CdO

Type	Donor NBO (i)	ED/e	Acceptor NBO (j)	ED/e	E$^{(2)}$ KJ/mol	E(j)-E(i) a.u.	F(i,j) a.u.
σ -σ*	BD (1)Zn1 - O3	1.89124	BD*(1)Zn1 - O3	0.08815	4.6	0.51	0.02
			BD*(1)Zn1 - O4	0.08815	28.87	0.51	0.05
			BD*(1)Cd2 - O3	0.08739	6.19	0.45	0.02
			BD*(1)Cd2 - O4	0.08739	8.28	0.45	0.03
σ -σ*	BD (1)Zn1 - O4	1.89124	BD*(1)Zn1 - O3	0.08815	28.87	0.51	0.05
			BD*(1)Zn1 - O4	0.08815	4.6	0.51	0.02
			BD*(1)Cd2 - O3	0.08739	8.28	0.45	0.03
			BD*(1)Cd2 - O4	0.08739	6.19	0.45	0.02
σ -σ*	BD (1)Cd2 - O3	1.87942	BD*(1)Zn1 - O3	0.08815	13.68	0.49	0.04
			BD*(1)Zn1 - O4	0.08815	11.88	0.49	0.03
			BD*(1)Cd2 - O3	0.08739	8.62	0.42	0.03
			BD*(1)Cd2 - O4	0.08739	25.4	0.42	0.05
σ -σ*	BD (1)Cd2 - O4	1.87942	BD*(1)Zn1 - O3	0.08815	11.88	0.49	0.03
			BD*(1)Zn1 - O4	0.08815	13.68	0.49	0.04
			BD*(1)Cd2 - O3	0.08739	25.4	0.42	0.05
			BD*(1)Cd2 - O4	0.08739	8.62	0.42	0.03
n -σ*	LP (1) O 3	1.97105	BD*(1)Zn1 - O3	0.08815	6.44	1.02	0.04
n -σ*	LP (1) O 4	1.97105	BD*(1)Zn1 - O4	0.08815	6.44	1.02	0.04

3.4. Frontier molecular orbitals

The frontier molecular orbitals, HOMO and LUMO determine the way, how the molecule interacts with other species and helps to characterize the chemical reactivity and kinetic stability of the molecule (Fleming, 1976). HOMO energy determines the ability to donate an electron and LUMO energy determines the ability to accept an electron. The energy gap between the HOMO and LUMO is very important in determining the chemical reactivity of a molecule. A small energy gap (HOMO–LUMO) implies low kinetic stability (Diener & Alford, 1998).

From Fig. 2 shows that the HOMO and Lumo electrons (Green and Red colors) are partially occupied for the whole of the molecule. The HOMO energy lies at -6.14129 eV and the LUMO energy lies at -3.74763 eV. The energy difference between the HOMO and LUMO was obtained as 2.39366 eV in the gas phase calculations. The small energy gap, it can be observed that the title molecule has low kinetic stability and high chemical reactivity. The FMO energies are listed in Table 4. In addition the DOS spectrum identified the energy level (occupied and virtual) of the title molecule as shown in Fig. 3.
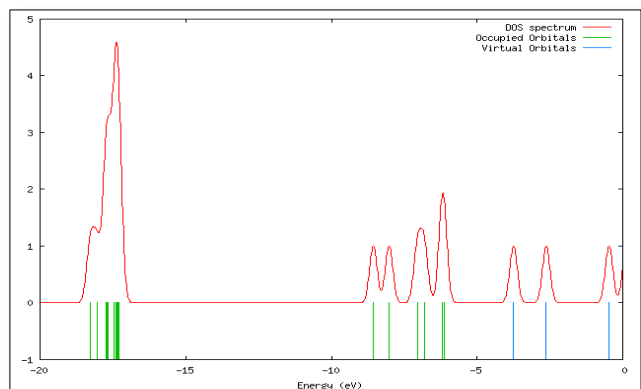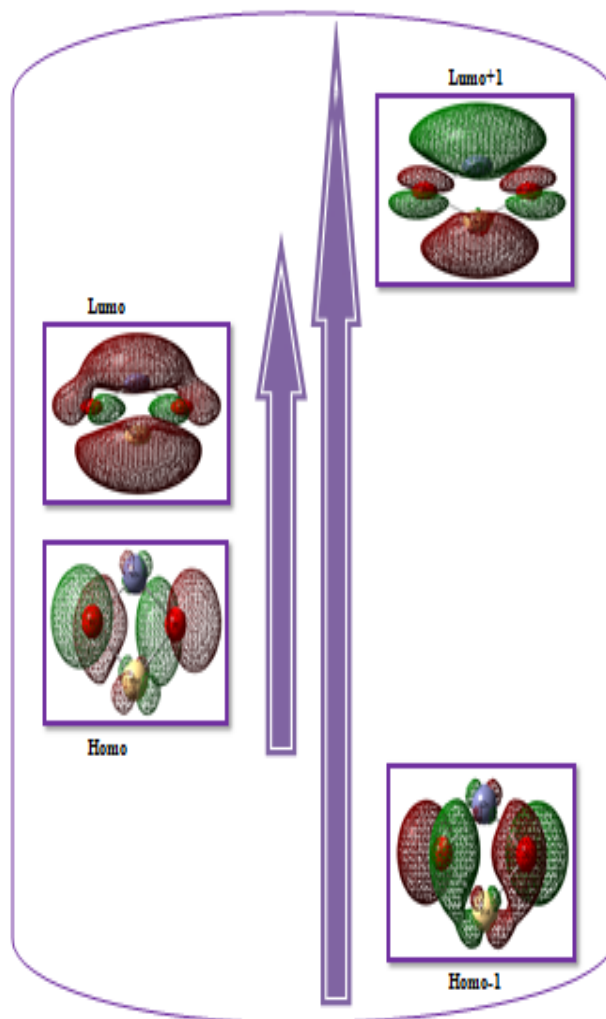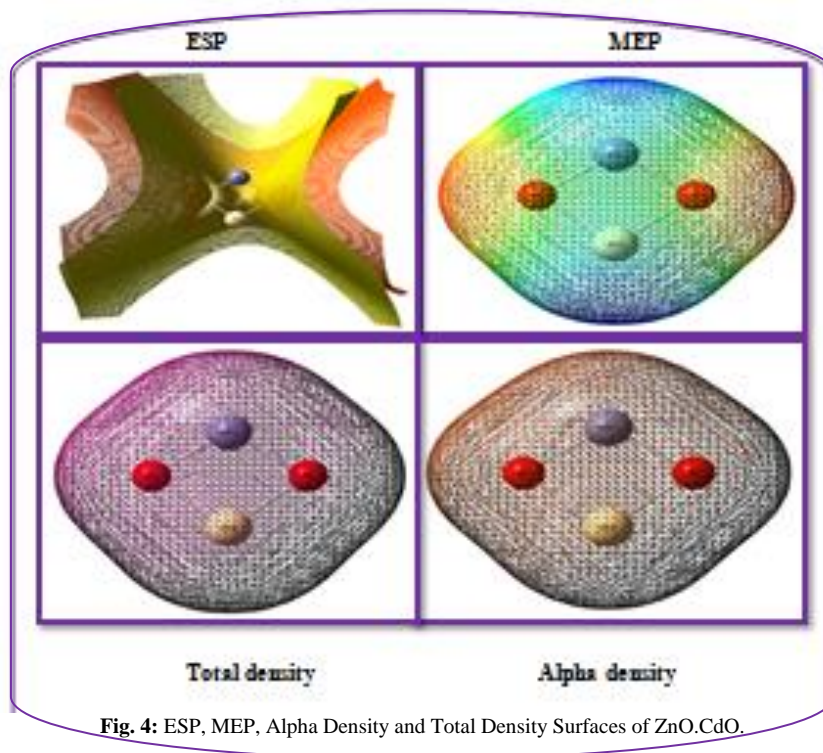

Fig. 3: DOS Spectrum of ZnO.CdO.

Fig. 2: The Homo-Lumo Diagram of ZnO.CdO.

Table 4: The Frontier Molecular Orbitals Energies of Zno.Cdo

Orbitals	Energies (a.u.)	Energies (eV)
Homo-1	-0.22806	-6.20551
Homo	-0.22570	-6.14129
Energygap	0.08797	2.39366
Lumo	-0.13773	-3.74763
Lumo+1	-0.09650	-2.62576

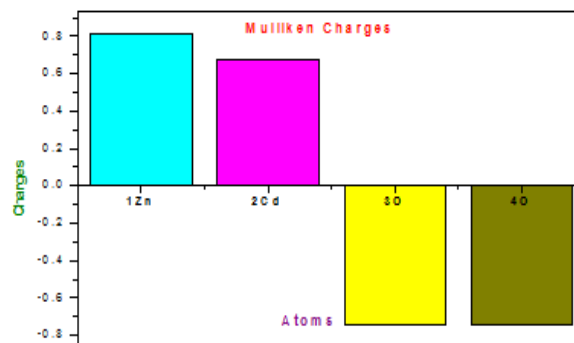**Fig. 4:** ESP, MEP, Alpha Density and Total Density Surfaces of ZnO.CdO.

3.5. MEP analysis

The molecular electrostatic potential (MEP) is related to the electron density and is a very useful descriptor for determining sites for electrophilic attack and nucleophilic reactions as well as hydrogen-bonding interactions (Scrocco & Tomasi, 1978; Okulik & Jubert, 2005). To predict reactive sites for electrophilic and nucleophilic attack for ZnO.CdO was calculated at B3LYP/LANL2DZ method. The electrophilic (negative-red color) and the nucleophilic (positive-blue color) reactivity are shown in Fig. 4. The different values of the electrostatic potential at the surface are represented by different colors; red represents regions of most electro negative electrostatic potential, blue represents regions of most positive electrostatic potential and green represents regions of zero potential. The electrostatic potential increases in the order red < orange < yellow < green < blue (Thul et al., 2010).

From Fig. 4 the negative region is mainly localized over the oxygen atoms. The positive surface mapped at Zn and Cd atoms behaves the heavy metals. The predominance of the green region in the MEP surface corresponds to a potential halfway between the two extreme regions red and blue color.

3.6. Mulliken charges

The Mulliken populations show one of the simplest pictures of charge distribution. The Mulliken charges provide net atomic populations in the molecule while electrostatic potentials yield the electric field out of the molecule produced by the internal charge distribution. The charge distributions are calculated at B3LYP/LANL2DZ method and the charges are listed in Table 5. The corresponding Mulliken's plot is shown in Fig. 5.

Fig. 5: Mulliken Atomic Charges of ZnO.CdO.

Table 5: The Mulliken Atomic Charges of ZnO.CdO.

Atoms	Charges
1Zn	0.81111
2Cd	0.67388
3O	-0.74249
4O	-0.74249

The metal (Zn1 and Cd2) atoms have more positive charges, which a group of inorganic material. The most negative charges were observed at O3 and O4 atoms, which may be due to the electro negativity atom.

3.7. Thermodynamic properties

The statistical thermo chemical analysis of ZnO.CdO is carried out considering the molecule to be at room temperature of 298.15 K and one atmospheric pressure. The thermodynamic functions such

as entropy (S), heat capacity at constant pressure (Cp) and enthalpy (ΔH) for various ranges (100–1000 K) of temperatures are determined and these results are presented in the Table 6. From Table 6, it can be observed that these thermodynamic functions are increasing with temperature ranging from 100 to 1000 K due to the fact that the molecular vibrational intensities increase with temperature (Ott & Boerio-Goates, 2000). The correlations between thermodynamic functions with temperatures are graphically represented in Fig. 6. All the thermodynamic data supply will be helpful information for the further study on the ZnO.CdO. It can be used to compute the other thermodynamic energies according to relationships of thermodynamic functions and estimate directions of chemical reactions according to the second law of thermodynamics in thermochemical field.
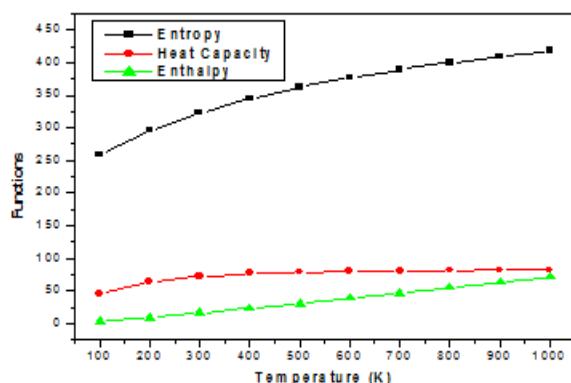

Fig. 6: Thermodynamic Functions and Temperatures of ZnO.CdO.

Table 6: The Thermodynamic Properties at Different Temperatures of ZnO.CdO

T (K)	S (J/mol.K)	Cp (J/mol.K)	ΔH (kJ/mol)
100	257.94	44.9	3.64
200	295.5	63.75	9.17
298.2	322.82	72.51	15.91
300	323.26	72.61	16.05
400	344.79	76.73	23.54
500	362.16	78.88	31.33
600	376.66	80.12	39.29
700	389.08	80.89	47.34
800	399.91	81.4	55.46
900	409.52	81.76	63.61
1000	418.15	82.02	71.8

4. Conclusion

The *ab initio* calculation of ZnO/CdO material was carried out for the first time in DFT study. The optimized geometrical parameters were calculated at DFT/B3LYP/LANL2DZ basis set. The bond angle of O3-Zn1-O4 (109.6677°) which is positively (~9°) deviated to O3-Cd2-O4 (100.0065°). This result shows that Zinc-oxygen bond as strong compared to Cadmium-oxygen bond in the present system. The β_0 value (2.57815 x10^{-30}esu) shows that the good NLO activity of the title molecule. The less energy gap of HOMO-LUMO is 2.39366 eV, which explain the eventual charge transfer occur within the molecule and it has more optical property. MEP surface predicts that the reactive sites of atoms due to the electrophilic attack and nucleophillic attack of the present material. The Mulliken atomic charges of ZnO/CdO has been calculated and also plotted. In addition thermodynamic properties of the title molecule have been also calculated.

REFERENCES

[1] Chong, X., Li, L., Yan, X., Hu, D., Li, H., & Wang, Y. (2012). Synthesis, characterization and room temperature photoluminescence properties of Al doped ZnO nanorods. Physica E: Low-Dimensional Systems and Nanostructures, 44(7-8), 1399–1405. https://doi.org/10.1016/j.physe.2012.03.001.

[2] Tsai, D.-S., Lin, C.-A., Lien, W.-C., Chang, H.-C., Wang, Y.-L., & He, J.-H. (2011). Ultra-High-Responsivity Broadband Detection of Si Metal–Semiconductor–Metal SchottkyPhotodetectors Improved by ZnO Nanorod Arrays. ACS Nano, 5(10), 7748–7753. https://doi.org/10.1021/nn203357e.

[3] Zhang, J., Wang, S., Xu, M., Wang, Y., Zhu, B., Zhang, S., & Wu, S. (2009). Hierarchically Porous ZnO Architectures for Gas Sensor Application. Crystal Growth & Design, 9(8), 3532–3537. https://doi.org/10.1021/cg900269a.

[4] Wang, L., Lou, Z., Fei, T., & Zhang, T. (2012). Templating synthesis of ZnO hollow nanospheres loaded with Au nanoparticles and their enhanced gas sensing properties. Journal of Materials Chemistry, 22(11), 4767-4771.https://doi.org/10.1039/c2jm15342d.

[5] Na, C. W., Woo, H.-S., Kim, I.-D., & Lee, J.-H. (2011). Selective detection of NO₂ and C₂H₅OH using a Co3O4-decorated ZnO nanowire network sensor. Chemical Communications, 47(18), 5148-5150.https://doi.org/10.1039/c0cc05256f.

[6] Wen, W., Wu, J.-M., & Wang, Y.-D. (2013). Gas-sensing property of a nitrogen-doped zinc oxide fabricated by combustion synthesis. Sensors and Actuators B: Chemical, 184, 78–84. https://doi.org/10.1016/j.snb.2013.04.052.

[7] Jayakrishnan, R., & Hodes, G. (2003). Non-aqueous electrodeposition of ZnO and CdO films. Thin Solid Films, 440(1-2), 19–25. https://doi.org/10.1016/S0040-6090(03)00811-3.

[8] Kanjwal, M. A., Barakat, N. A. M., Sheikh, F. A., & Kim, H. Y. (2009). Electronic characterization and photocatalytic properties of TiO2/CdO electrospunnanofibers. Journal of Materials Science, 45(5), 1272–1279. https://doi.org/10.1007/s10853-009-4078-3.

[9] Karami, H. (2010). Investigation of sol-gel synthesized CdO-ZnO nanocomposite for CO gas sensing. Int. J. Electrochem. Sci, 5, 720-730.

[10] Frisch, M.J., Trucks, G.W., Schlegel, H.B., Scuseria, G.E., Robb, M.A. (2004). Theoretical and Computational Aspects of Magnetic Organic Molecules. Gaussian Inc, Wallingford, CT.

[11] Schlegel, H. B. (1982). Optimization of equilibrium geometries and transition structures. Journal of Computational Chemistry, 3(2), 214–218. https://doi.org/10.1002/jcc.540030212.

[12] Scott, A. P., & Radom, L. (1996). Harmonic Vibrational Frequencies: An Evaluation of Hartree−Fock, Møller−Plesset, Quadratic Configuration Interaction, Density Functional Theory, and Semiempirical Scale Factors. The Journal of Physical Chemistry, 100(41), 16502–16513. https://doi.org/10.1021/jp960976r.

[13] Irikura, K.K. (2002). THERMO.PL, National Institute of Standards and Technology.

[14] Andraud, C., Brotin, T., Garcia, C., Pelle, F., Goldner, P., Bigot, B., & Collet, A. (1994). Theoretical and experimental investigations of the nonlinear optical properties of vanillin, polyenovanillin, and bisvanillin derivatives. Journal of the American Chemical Society, 116(5), 2094–2102. https://doi.org/10.1021/ja00084a055.

[15] Zhang, C. R., Chen, H. S., & Wang, G. H. (2004). Chem. Res. Chin, 20, 640-646.

[16] Kleinman, D. A. (1962). Nonlinear Dielectric Polarization in Optical Media. Physical Review, 126(6), 1977–1979. https://doi.org/10.1103/PhysRev.126.1977.

[17] Reed, A. E., & Weinhold, F. (1983). Natural bond orbital analysis of near-Hartree–Fock water dimer. The Journal of Chemical Physics, 78(6), 4066–4073. https://doi.org/10.1063/1.445134.

[18] Reed, A. E., & Weinhold, F. (1985). Natural localized molecular orbitals. The Journal of Chemical Physics, 83(4), 1736–1740. https://doi.org/10.1063/1.449360.

[19] Reed, A. E., Weinstock, R. B., & Weinhold, F. (1985). Natural population analysis. The Journal of Chemical Physics, 83(2), 735–746. https://doi.org/10.1063/1.449486.

[20] Foster, J. P., & Weinhold, F. (1980). Natural hybrid orbitals. Journal of the American Chemical Society, 102(24), 7211–7218. https://doi.org/10.1021/ja00544a007.

[21] Chocholoušová, J., Špirko, V., & Hobza, P. (2004). First local minimum of the formic acid dimer exhibits simultaneously red-shifted O–H···O and improper blue-shifted C–H···O hydrogen bonds. Phys. Chem. Chem. Phys., 6(1), 37–41. https://doi.org/10.1039/B314148A.

[22] Fleming, I. (1976). Frontier Orbitals and Organic Chemical Reactions, John Wiley and Sons, New York, 5–27.

[23] Diener, M. D., & Alford, J. M. (1998). Isolation and properties of small-bandgap fullerenes. Nature, 393 (6686), 668–671. https://doi.org/10.1038/31435.

[24] Scrocco, E., & Tomasi, J. (1978). Electronic molecular structure, reactivity and intermolecular forces: a neuristic interpretation by means of electrostatic molecular potentials. In Advances in

quantum chemistry, 11, 115-193. https://doi.org/10.1016/S0065-3276(08)60236-1.

[25] Okulik, N., & Jubert, A. H. (2005). Theoretical analysis of the reactive sites of non-steroidal anti-inflammatory drugs. Internet Electronic Journal of Molecular Design, 4(1), 17-30.

[26] Thul, P., Gupta, V. P., Ram, V. J., & Tandon, P. (2010). Structural and spectroscopic studies on 2-pyranones. Spectrochimica Acta Part A: Molecular and Biomolecular Spectroscopy, 75(1), 251–260. https://doi.org/10.1016/j.saa.2009.10.020.

[27] Ott, J. B., & Boerio-Goates, J. (2000). Introduction. Chemical Thermodynamics: Principles and Applications, 1–36. https://doi.org/10.1016/B978-012530990-5/50002-X.